Supporting Information

MOF-Derived Co-Mo Bimetallic Heterostructures for Selective Trapping and Conversion of Polysulfides in Lithium-Sulfur Batteries

Rongmei Zhu[1,*], Yuxuan Jiang[1], Bingxin Sun[1], Wang Zhang[1,2] and Huan Pang[1,*]

1. School of Chemistry and Chemical Engineering, Yangzhou University, Yangzhou, Jiangsu, 225009, P. R. China
2. Research Institute for Convergence Science, Seoul National University, Seoul, 08826, Republic of Korea

* Corresponding author

E-mail addresses:

rmzhu@yzu.edu.cn (R. Zhu)

panghuan@yzu.edu.cn, huanpangchem@hotmail.com (H. Pang)

Homepage: https://www.x-mol.com/groups/panghuan

Contents

1. Experimental section

1.1 Chemicals and reagents

Cobalt nitrate (99.99%, AR), 2-methylimidazole (2-HmIm), urea and sublimed sulfur powder were obtained from Aladdin (China), $Na_2MoO_4 \cdot 2H_2O$, Thioacetamide (TAA), Super P and Methanol (99.5%, AR) were purchased from Shanghai Chemical Reagents Company (Shanghai, China).

1.2 Materials synthesis

1.2.1 Synthesis of ZIF-67

Synthesis of ZIF-67: 8.6 mmol of $Co(NO)_3 \cdot 6H_2O$ was weighed along with 34.3 mmol of 2-HmIm, and each of them was dissolved in 100 ml of CH_3OH. The solution was ultrasonicated for 20 min to disperse homogeneously, and the Co metal source solution was rapidly poured into the ligand solution at room temperature with magnetic stirring for 1 min, and then left to stand for 24 h. The purple product was collected by centrifugation and washed with methanol for three times. Subsequently, the products were dried in an oven at 60 ℃ for 12 h for subsequent use.

1.2.2 Synthesis of PR1

80 mg of ZIF-67 was dissolved in 40 ml of ethanol, sonicated for 20

min to make it dispersed uniformly, and 40 mg of TAA was added and stirred for 10 min to make the solution mixed homogeneously, and then refluxed at 80 ℃ for 1 h. Centrifugation was performed and washed with ethanol, and the product was placed in an oven at 60 ℃ to dry for 12 h to obtain the PR1 powder.

1.2.3 Synthesis of PR2

75 mg of ZIF-67 was dissolved in 75 ml of ethanol, sonicated for 20 min to make it dispersed uniformly, and 75 mg of TAA was added and stirred for 10 min to make the solution mixed homogeneously, and then refluxed at 120 ℃ for 6 h. Centrifugation was performed and washed with ethanol, and the product was placed in an oven at 60 ℃ to dry for 12 h to obtain the PR2 powder.

1.2.4 Synthesis of ZIF-67@CoS_x/MoO_3 and CoS_x/MoO_3

100 mg of PR1 was dissolved in 40 ml of ethanol, sonicated for 20 min to make it dispersed uniformly, then 20 ml of $Na_2MoO_4 \cdot 2H_2O$ aqueous solution (0.02 mol/L) was added and stirred at room temperature for 2 h, after centrifugal drying of the solution to obtain ZIF-67@CoS_x/MoO_3. For comparison, CoS_x/MoO_3 was prepared by treating PR2 using the same process.

1.3 Preparation of modified separators and cathode

1.3.1 Preparation of modified separators

42 mg of CoS_x/MoO_3 powder and 6 mg of Super P were weighed and ground until homogeneous, then 125 mg of pre-formulated N-methyl-2-pyrrolidone (NMP) solution containing 5 wt.% polyvinylidene fluoride (PVDF) was added and applied to the surface of the PP separator using a tetrahedral spatula (set to a thickness of 25 μm). The separators were dried in a vacuum oven at 40 °C for 12 h. Finally, the separators were cut into 16 mm pieces. For comparison, ZIF-67@CoS_x/MoO_3/PP separators were also prepared by the same method.

1.3.2 Preparation of cathode

Super P/S composite was first prepared to used as the activated material of LSB through melt-diffusion method (Super P and sublimation of sulfur mixed uniformly into the hydrothermal reaction kettle sealed, warmed to 155 ℃ insulation 12h and the sulfur content of the sample is indicated in Fig S23. For the preparation of cathode, Super P/S, Super P, and NMP solution containing 5 wt.% PVDF (8:1:1 by weight) were milled together to form uniform slurry. Then, the slurry was coated on the carbon coated Al foil and dried in vacuum at 40 ℃ for 12 h. The obtained working electrodes were cut to circular electrode with a diameter of 12 mm. The

mass loading of active sulfur was about 1.1-1.3 mg cm^{-2}.

1.4 Materials Characterization

The Powder X-ray diffraction (PXRD) patterns were performed by Bruker AXS D8 advance with Cu Kα radiation of 40 kV (λ=1.5418 Å). Scanning electron microscopy (SEM) images were obtained by Zeiss-Supra 55 microscope. Transmission electron microscopy (TEM) and Energy Dispersive Spectrometer (EDS) elemental mapping scans were recorded using Tecnai G2 F30 S-TWIN at an acceleration voltage of 300 kV. Thermogravimetry analysis (TGA) was conducted with Diamond TG/DTA thermal analyzer (PerkinElmer, USA) to calculate the sulfur content of prepared samples. FT-IR measurement was investigated on a TENSOR27. X-ray photoelectron spectroscopy (XPS) analysis was carried out using a Thermo Scientific ESCALAB 250Xi X-ray photoelectron spectrometer with Al Kα radiation of 1486.6 eV as the excitation source. The survey thickness is 2-3 nm.

1.5 LiPSs adsorption test

For the adsorption test, 30 mg ZIF-67@CoS_x/MoO_3 or CoS_x/MoO_3 were soaked in 4 mL Li_2S_4 solution (10 mmol/L). The Li_2S_4 solution were prepared according to the reaction Equation S1:

$$3S + Li_2S \leftrightarrow Li_2S_4 \qquad (S1)$$

using a solvent mixture of 1,3-Dioxolane (DOL) and dimethoxyethane (DME) (1:1 in volume). For the in-situ adsorption experiment, 10mg ZIF-67@CoS_x/MoO_3 or CoS_x/MoO_3 were soaked in 1ml of Li_2S_4 and 2ml of DOL/DME solution (1:1 in volume). UV-vis spectra of the above solutions (diluted 5 times before testing) were recorded by using a UV2550 instrument (Shimadzu, Japan). The concentration variations in these solutions were detected by the UV-vis spectroscopy.

1.6 Li-S cell assembling and test:

The CR 2032-type coin cells were fabricated using the working electrode, lithium foil as the counter and anode electrode, Celgard 2400 as the separator. The electrolyte was used 1.0 mol L^{-1} lithium bis(trifluoromethanesulfonyl)imide (LiTFSI Sigma-Aldrich (USA), 99.95%) in DOL (Sigma-Aldrich (USA), 99.0%) and DME (Sigma-Aldrich (USA), 99.0% (volume ratio, 1:1) with 1 wt.% $LiNO_3$ in an argon-filled glove box (where both water and oxygen levels are below 0.1 ppm. The value of the electrolyte to S (E/S) ratio is 15 μL mg^{-1} (according to the weight of S). The GCD tests were estimated in the voltage window of 1.7 - 2.8 V. The rate capability was also tested by varying the current density from 0.1 C to 1 C (1 C = 1675 mAh g^{-1}) on a battery measurement system (CT2001A, Wuhan Land, China) at room temperature. CV and EIS curves

were measured on an electrochemical workstation (CHI660E, Chenhua, Shanghai, China). CV curves was performed from 2.8 V to 1.7 V (vs Li^+/Li) at a scanning rate of 0.1 mV s^{-1}, and the frequency of EIS was performed form 100 kHz to 0.01 Hz at open-circuit potential. For In situ EIS measurements, Li-S cells were discharged in galvanostatic mode at 0.1 C for 10 min, and then the cell was rest for 10 min to reach the quasi-open circuit voltage (QOCV). The EIS test is performed when the QOCV is slightly below the target voltage.

2. Supplementary images

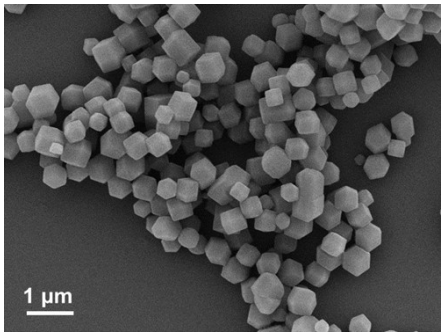

Fig. S1 SEM image of ZIF-67.

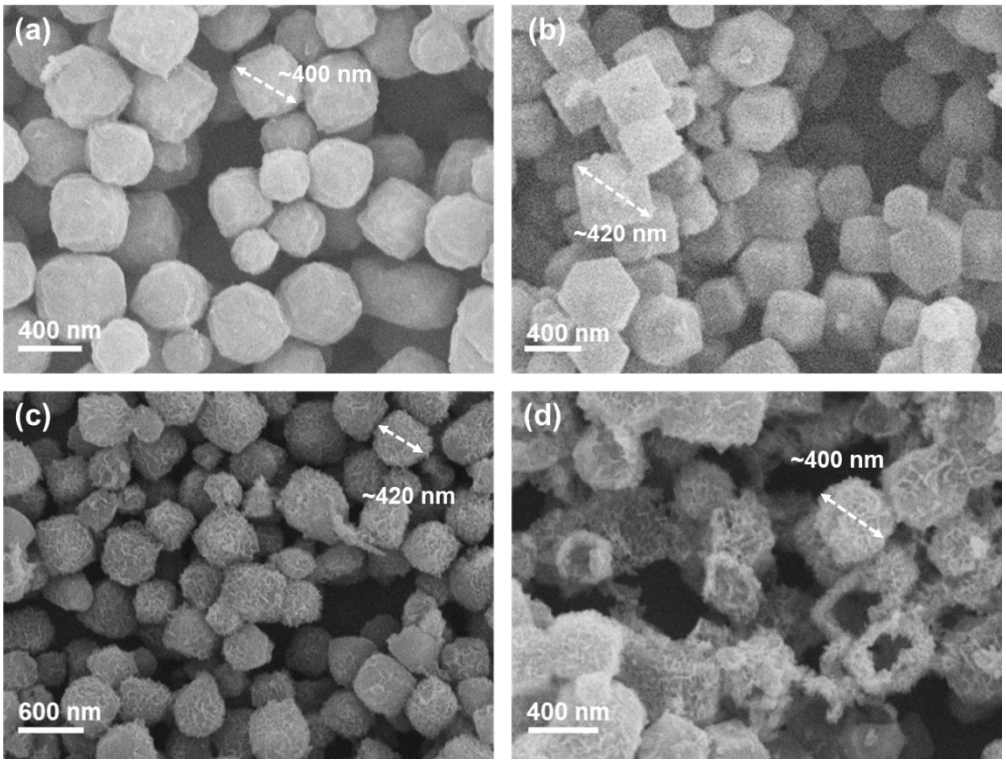

Fig. S2 The high-resolution SEM images of (a) PR1, (b) PR2, (c) ZIF-67@CoS_x/MoO_3 and (d) CoS_x/MoO_3.

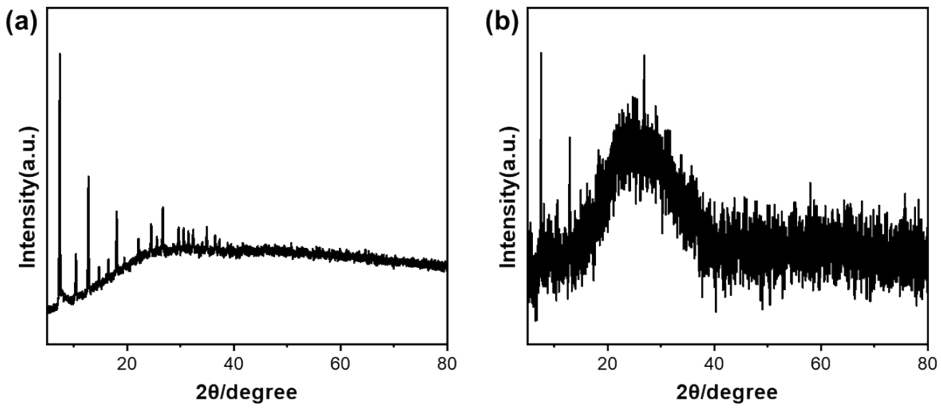

Fig. S3 The XRD patterns of (a) PR1 and (b) PR2.

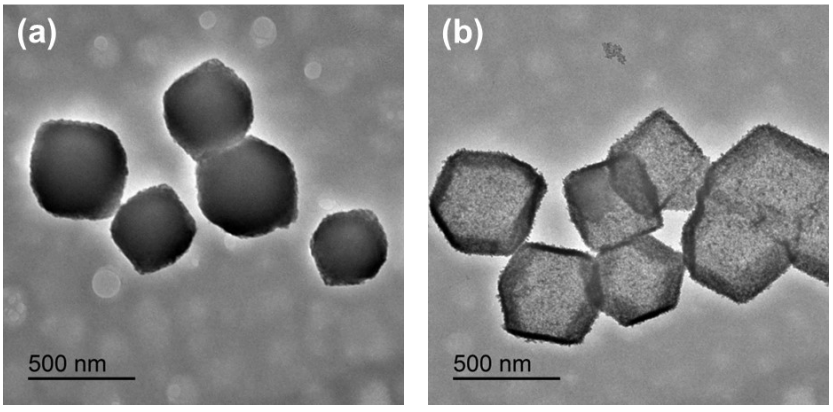

Fig. S4 TEM images of (a) PR1 and (b) PR2.

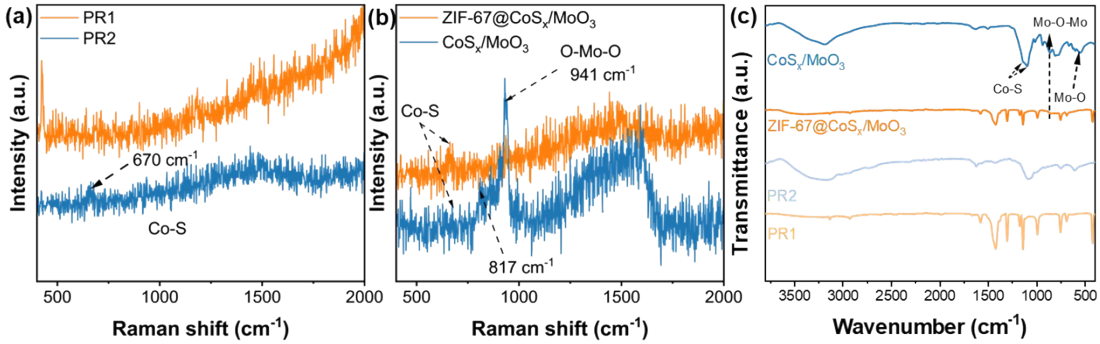

Fig. S5 Raman spectra of (a) PR1 and PR2, (b) ZIF-67@CoS_x/MoO_3 and CoS_x/MoO_3. (c) FTIR pattern of PR1 and PR2, ZIF-67@CoS_x/MoO_3 and CoS_x/MoO_3.

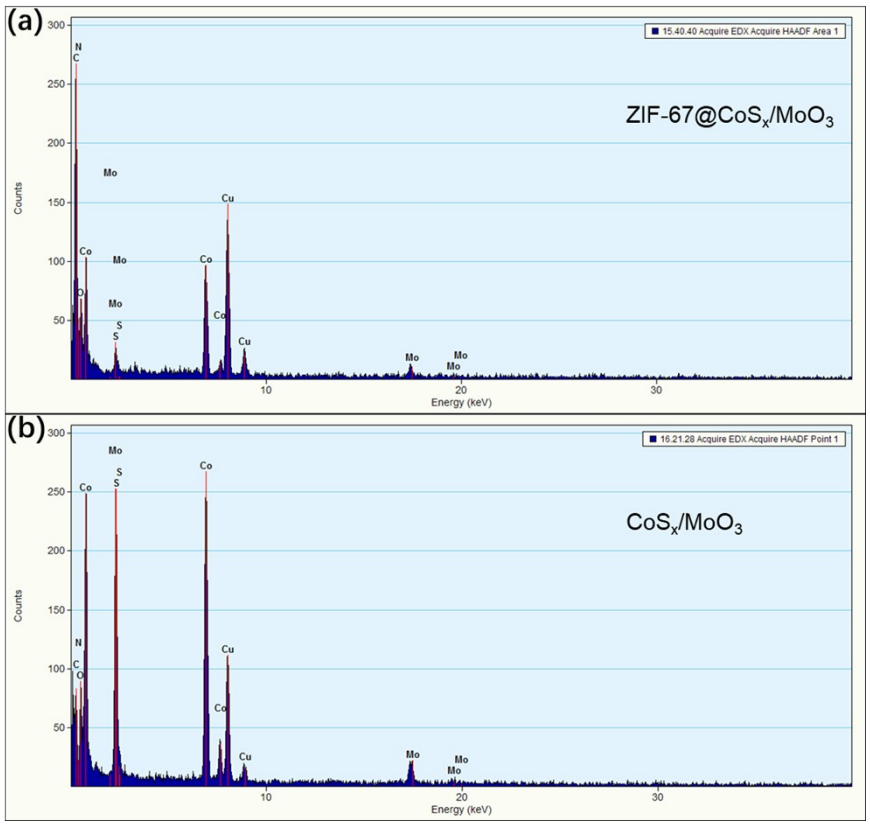

Fig. S6 EDX results of (a) ZIF-67@CoS_x/MoO_3 and (b) CoS_x/MoO_3.

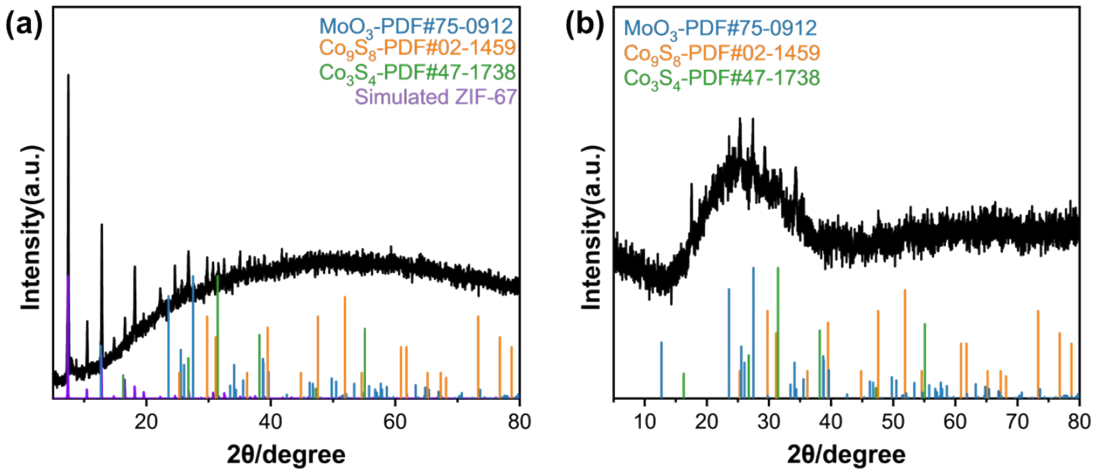

Fig. S7 The XRD patterns of (a) ZIF-67@CoS_x/MoO_3 and (b) CoS_x/MoO_3.

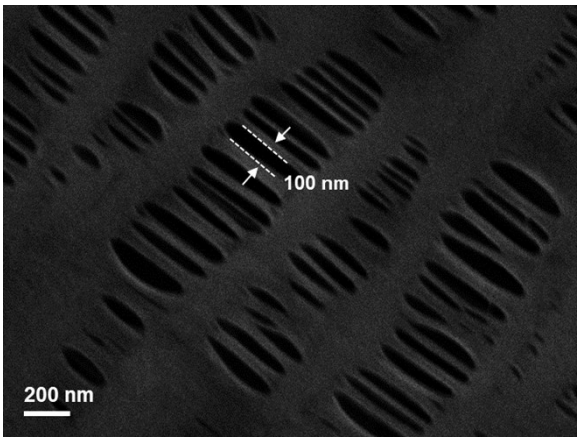

Fig. S8 The high-resolution SEM image of PP.

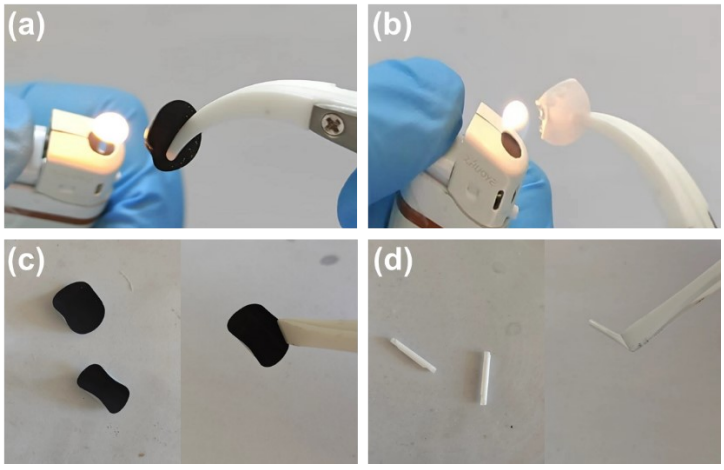

Fig S9. Optical photographs of modified separators as well as PP: (a-b) in combustion and (c-d) stored at 130 degrees Celsius for 10 min.

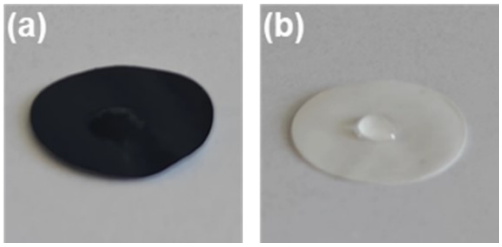

Fig. S10 Optical photos of electrolyte drops on the (a) modified separator and (b) PP.

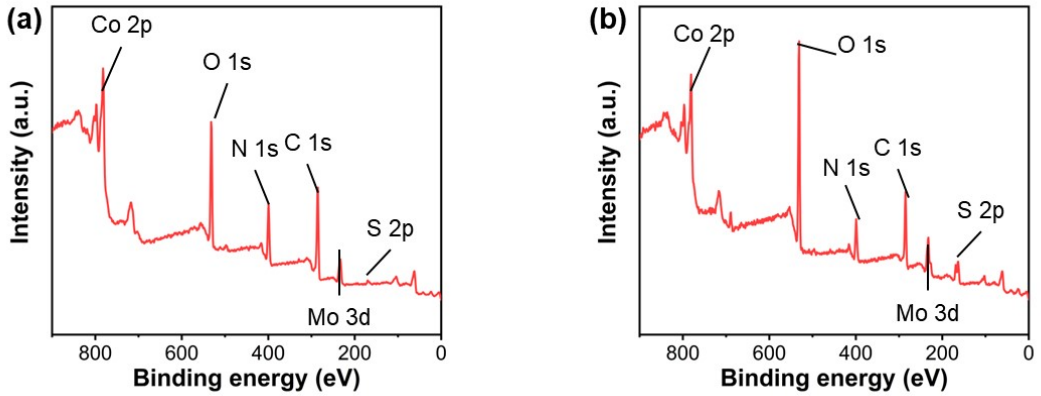

Fig. S11 Full XPS spectra of (a) ZIF-67@CoS_x/MoO_3, (b) ZIF-67@$CoS_x/MoO_3/Li_2S_4$.

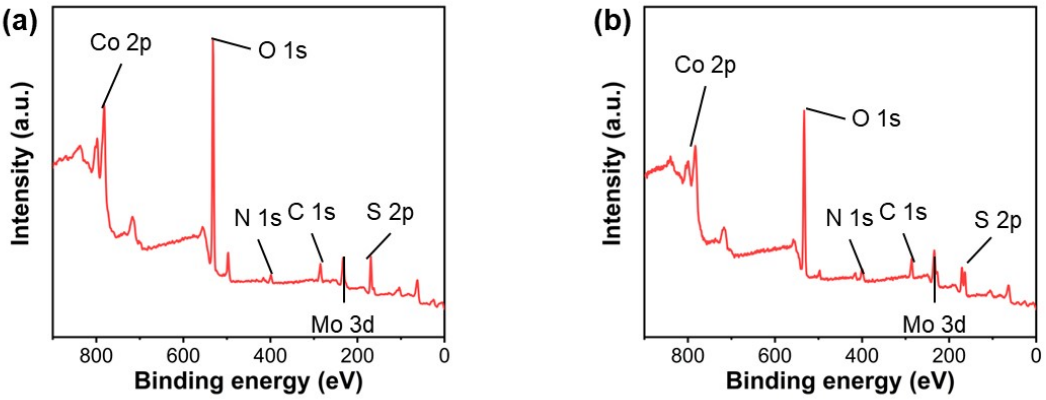

Fig. S12 Full XPS spectra of (a) CoS_x/MoO_3, (b) $CoS_x/MoO_3/Li_2S_4$.

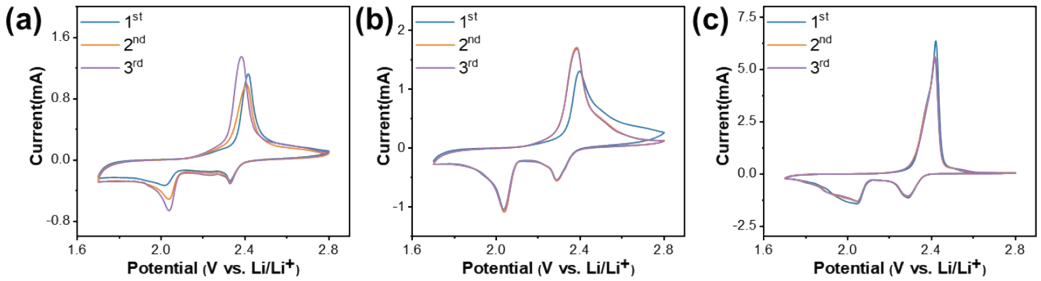

Fig. S13 3-turn CV curves of the battery with (a) PR1/PP, (b) PR2/PP, (c) ZIF-

67@CoS_x/MoO_3/PP.

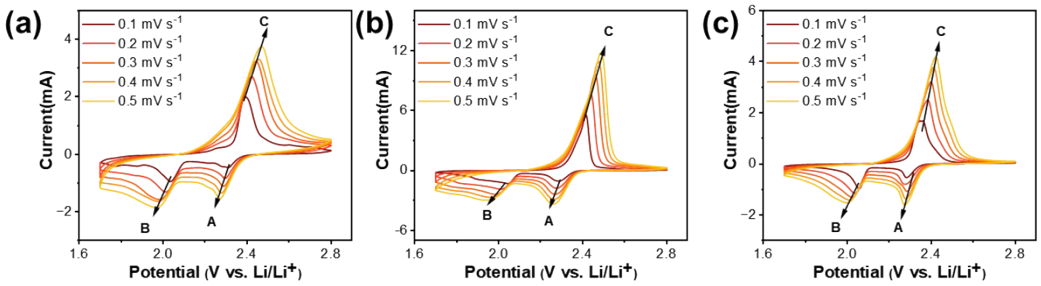

Fig. S14 The current response of the battery with (a) PR1/PP, (b) PR2/PP, (c) ZIF-67@CoS_x/MoO_3/PP.

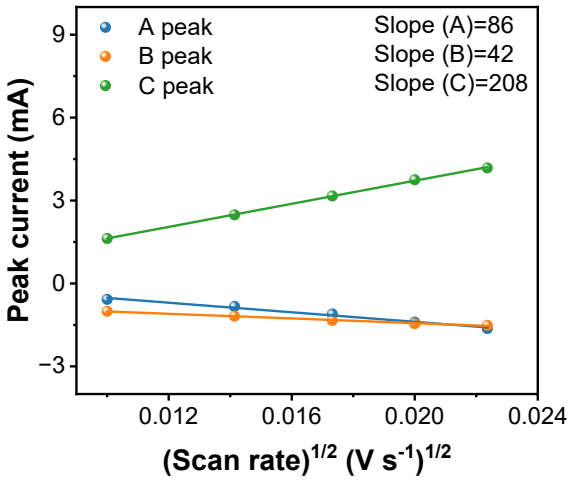

Fig. S15 The linear relationship of I_p and $v^{1/2}$ of LSBs with ZIF-67@CoS_x/MoO_3/PP.

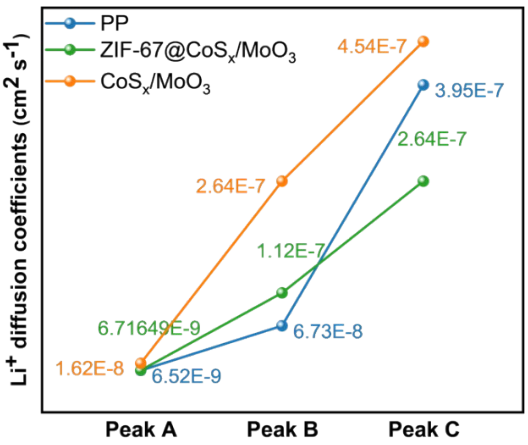

Fig. S16 Lithium-ion diffusion rate of batteries equipped with different separators.

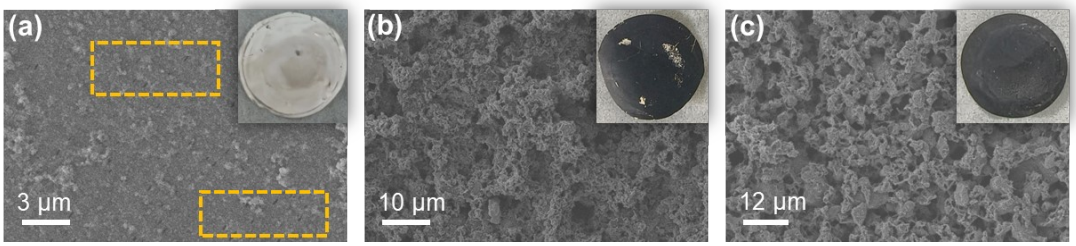

Fig. S17 SEM images of the diaphragm obtained by disassembling the cell after 100 cycles at a current of 0.2 C (inset shows the corresponding optical photograph): (a) PP, (b) ZIF-67@CoS_x/MoO_3/PP and (c) CoS_x/MoO_3/PP.

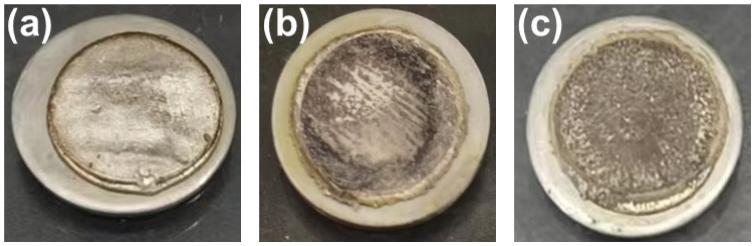

Fig. S18 The optical photos of the Li metal anodes after the cycling tests: (a) CoS_x/MoO_3, (b) ZIF-67@CoS_x/MoO_3, (c) PP.

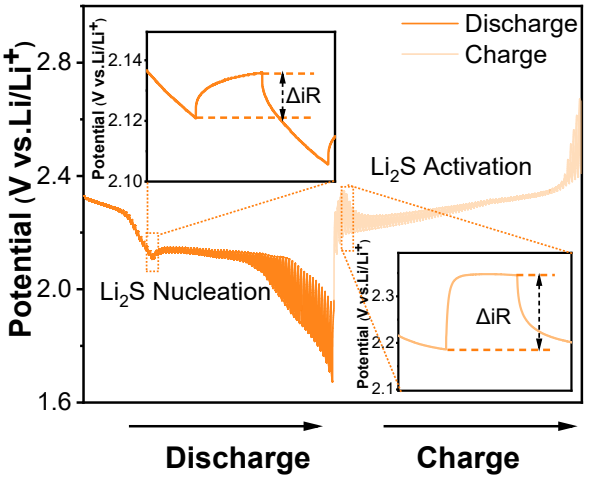

Fig. S19 GITT voltage profiles of ZIF-67@CoS_x/MoO_3/PP.

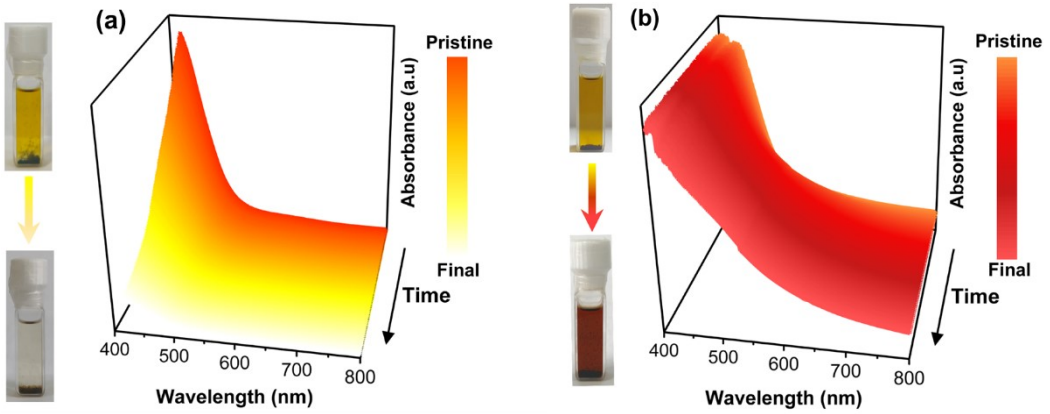

Fig. S20 In situ UV-vis spectra of (a) CoS_x/MoO_3, (b) ZIF-67@CoS_x/MoO_3.

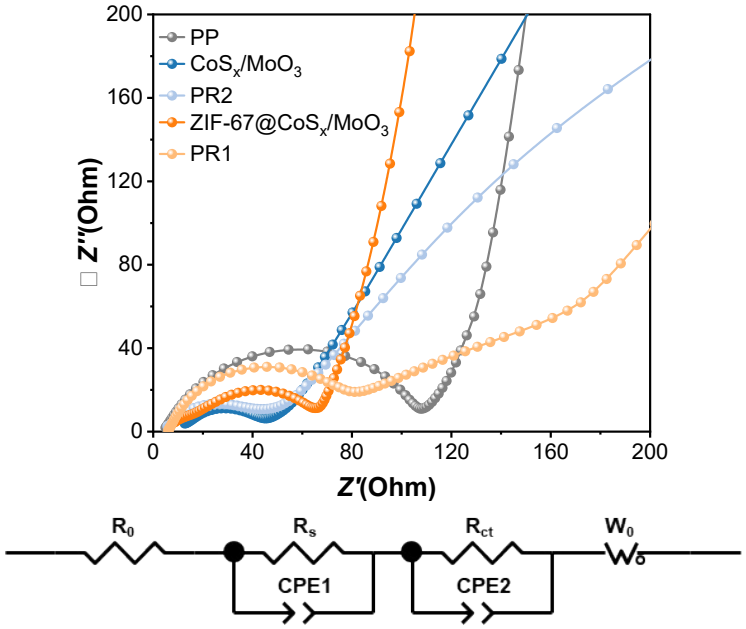

Fig. S21 Nyquist plots of batteries with different separators and the fitting circuit diagram of the Nyquist curve.

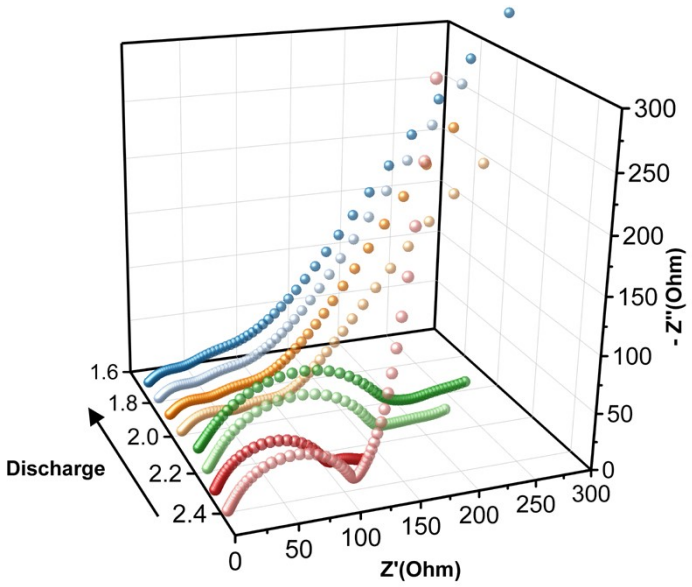

Fig. S22 In-situ EIS spectra of the battery with ZIF-67@CoS_x/MoO_3/PP.

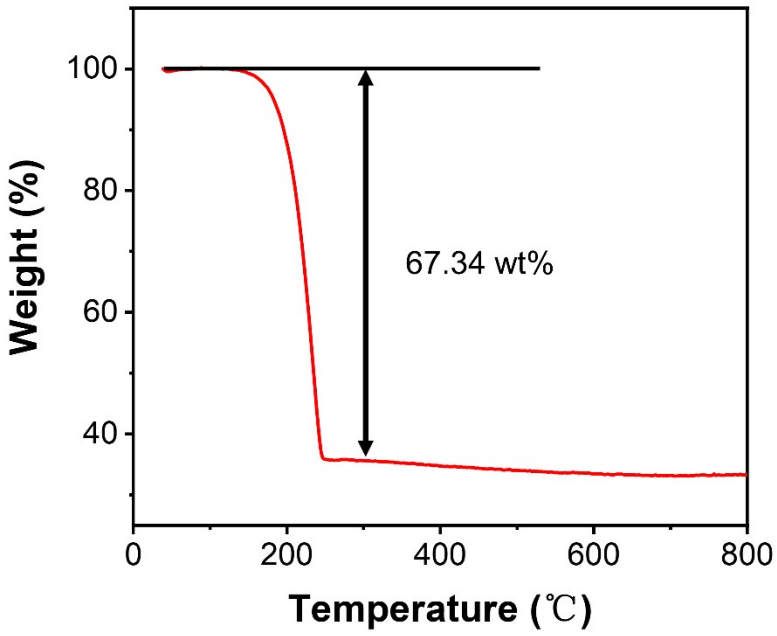

Fig. S23 TGA curve of the Super P/S.

3. Supplementary table

Table S1. Electrochemical performance of the Li-S batteries with various modified separators.

Modified materials	Sulfur loading (mg cm^{-2})	Rates/Cycle numbers	Discharge capacity (mAh g^{-1})	Decay rates (%)	Ref.
CoS_x/MoO_3/PP	1.1~1.3	1C/500	681	0.041%	This work
Co_9S_8 Nano-flower	1.1	0.2C/800	665	0.049%	[1]
Co_9S_8 Nanorods	3.0	0.5C/350	612	0.024%	[2]
1T MoS_2@CNT	0.8	1C/500	670	0.052%	[3]
MoS_2 QDs-NRGO	2.0	0.2C/180	1126	0.16%	[4]
CoS_2/NC@1T MoS_2	0.8	1C/500	953	0.07%	[5]
Mo_2C/MoO_3	3.5	0.5C/300	972	0.063%	[6]
MoO_3@CNT	1.0	0.3C/200	755	0.19%	[7]
Co@N-CNTs/N-Mo_xC	1.0	1C/500	610	0.09%	[8]
Co/Mo_2C@CNTs	1.0	1C/600	1186	0.07%	[9]

4. Reference

[1]Q. Wang, H. Zhao, B. Li, C. Yang, M. Li, Y. Li, P. Han, M. Wu, T. Li, R. Liu, MOF-derived Co_9S_8 nano-flower cluster array modified separator towards superior lithium sulfur battery, Chin. Chem. Lett. 32 (2021) 1157–1160. https://doi.org/10.1016/j.cclet.2020.09.022.

[2]F. Wang, J. Qian, Y. Li, K. Yu, L. Li, F. Wu, R. Chen, Co_9S_8 Nanorods as an Electrocatalyst To Enhance Polysulfide Conversion and Alleviate Passivation in Li–S Batteries under Lean Electrolyte Conditions, ACS Appl. Mater. Interfaces 12 (2020) 21701–21708. https://doi.org/10.1021/acsami.0c03750.

[3]Y.C. Jeong, J.H. Kim, S.H. Kwon, J.Y. Oh, J. Park, Y. Jung, S.G. Lee, S.J. Yang, C.R. Park, Rational design of exfoliated 1T MoS_2 @CNT-based bifunctional separators for lithium sulfur batteries, J. Mater. Chem.a 5 (2017) 23909–23918. https://doi.org/10.1039/C7TA08153G.

[4]J. Zhang, J. Hu, X. Li, L. Yang, L. Yang, J. Lin, J. Huang, G. Xu, High-performance MoS_2 quantum dots/graphene functionalized separator and its failure analysis under high sulfur loading, Chemical Engineering Journal 456 (2023) 140972. https://doi.org/10.1016/j.cej.2022.140972.

[5]Q. Li, H. Liu, B. Jin, L. Li, Q. Sheng, M. Cui, Y. Li, X. Lang, Y.

Zhu, L. Zhao, Q. Jiang, Anchoring polysulfides *via* a CoS_2/NC@1T MoS_2 modified separator for high-performance lithium–sulfur batteries, Inorg. Chem. Front. 10 (2023) 959–971. https://doi.org/10.1039/D2QI01884E.

[6]C. Zhao, S. Xu, X. Zhang, Y. Wang, P. Rui, J. Zheng, C. Zhao, Construction of nanoporous Mo_2C shell/MoO_3 core composite by converting MoO_3 and its superior performance in lithium sulfur battery, J. Electroanal. Chem. 922 (2022) 116742. https://doi.org/10.1016/j.jelechem.2022.116742.

[7]L. Luo, X. Qin, J. Wu, G. Liang, Q. Li, M. Liu, F. Kang, G. Chen, B. Li, An interwoven MoO_3@CNT scaffold interlayer for high-performance lithium–sulfur batteries, J. Mater. Chem. A 6 (2018) 8612–8619. https://doi.org/10.1039/C8TA01726C.

[8]G. Zhao, S. Liu, X. Zhang, Y. Zhang, H. Shi, Y. Liu, L. Hou, C. Yuan, Construction of Co@N-CNTs grown on N-Mo_x C nanosheets for separator modification to enhance adsorption and catalytic conversion of polysulfides in Li–S batteries, J. Mater. Chem.a 11 (2023) 1856–1865. https://doi.org/10.1039/D2TA09123B.

[9]W. Liu, M. Lei, X. Zhou, C. Li, Heterojunction interlocked catalysis-conduction network in monolithic porous-pipe scaffold for endurable Li-S batteries, Energy Storage Materials 58 (2023) 74–84. https://doi.org/10.1016/j.ensm.2023.03.004.